Super High Vertical Resolution Non-Contact 3D Surface Profiler by Focus Variation with White Light Interferometry

Takashi NISHIKAWA

Nikon Corporation, Chiyoda-ku, Tokyo 100-8331, Japan, Takashi.Nishikawa@nikon.com

Abstract:
This system is developed as a focus variation microscopic system with great versatility and high vertical resolution. Conventional focus variation microscopic systems cannot measure surface topography of smooth surfaces such as a glass surface because the surface has no texture to get effective point focus sharpness. This system can obtain very high point focus sharpness by operating a 3x3x3 voxel operator, we call 'the Digital Stylus', to fringe images which are generated by the two beam interferometric objective lens. Furthermore a new algorithm to decide the position of focal point, we call 'the APF: Approaching Function' method, is introduced. The decision of the focal position for each pixel is made by Newton's method with this APF. As 1 pico meter is set for the truncation error of Newton's method the system can calculate the surface topography with 1 pico meter vertical resolution. The traceability of surface topography data using an 8nm Standard Step Height Sample certified by NIST is shown in this paper. Sample data of a super smooth SiC wafer are also presented. This system allows us to get surface topography data by scanning once while other White Light Interferometry Systems require many scans for averaging to reduce the system noise. Not only will it measure super smooth surfaces but also very rough surfaces such as a ceramic bump without any changes of system configuration or parameters. This system will contribute significantly to the efficiency of the study of materials science.

Keywords: Surface Profiler, Focus Variation, White Light Interferometry, Approaching Function, SiC Wafer

1. INTRODUCTION

Surface metrology systems using the technology of Focus Variation (hereinafter, abbreviated as FV) has been developed and applied in the fields of engineering and materials science such as cutting-tool, precision manufacturing, automotive industry, electronics and paper industry. [1] One of the major advantages of microscopic systems using this method is that it can measure steep flanks or very rough surfaces. Also, it can create all-in-focused images with very good quality because it can use bright field objective lenses which are dedicated for microscopic imaging. On the other hand surfaces which have no microscopically visible texture such as glass surfaces or mirror polished metal surfaces are not able to be measured with very good quality. Another disadvantage is that the vertical resolution is dependent on the focus depth of the objective lens. For example, focus depth of a typical 2.5X objective lens is over 45μm. That meaning is that there is no significant focus variation within 45μm. These features may be major reasons for limitation of expanding into applicable fields for the system with this technology.

In 1985 J. C. Wyant and et al developed the microscopic system with technology of PSI (Phase Shifting Interferometry) and applied it to the evaluation of magnetic tape surfaces. [2] This method and system allows us to measure super smooth surfaces such as glass surfaces or polished metal surfaces, which are not able to be measured by the FV and system. This White Light Interferometry (hereinafter, abbreviated as WLI) early system was limited to measurements of smooth surfaces. Many researchers have contributed to the expansion of WLI in the years since then. Now there are FDA [3], WLPSI [4] and CCI [5] technologies and systems. The WLI has advantages in that it can measure smooth surfaces. However, the result of surface topography, in some cases, may be affected by the NA (Numerical Aperture) of lens or by the fluctuation of average wavelength of the illuminator. So the correction and calibration of the height data are required frequently in some of the WLI systems.

The Focus Variation with White Light Interferometry (hereinafter, abbreviated as FVWLI) is proposed as a new algorithm for measurement of surface topography. The FVWLI covers disadvantages in the FV and WLI without losing the major advantages.

2. METHODS

2.1 System Configuration

In this section, the configuration of the microscope system and fundamentals of interferometry are described as a premise of the algorithms explained in the following sections. A photograph of system type BW-S507 is shown in Fig. 1. The feature drawing of the microscope, which is designed for the BW-S500 series, is also shown in Fig. 2. A concept drawing of optics system is in Fig. 3. The white light interferometric microscope can be realized by equipping the two-beam interferometric objective lens in a conventional optical microscope. The parallel luminous flux made by the LED light source and the illuminator is split into two optical fluxes of nearly equal intensity by the half mirror. One of these fluxes directed onto a reference mirror and the other onto the specimen. The optical flux reflected on the reference mirror and the flux reflected on the specimen, these two optical fluxes go into the imaging area of the camera. The optical interference pattern is observed by the camera because these two fluxes are originated from the same optical waves.

The concept of 'the Interferogram', which is generally used in the white light interferometry, is explained as follows: the focus point is varied by z-scanning using the Piezo actuator which is mounted between the nosepiece and the illuminator. During the z-scanning the intensity values measured by the camera is saved to the memory in the computer. So we can handle time-base pixel data as voxel data of 3D space coordination. The graph with the intensity value as the horizontal axis and z coordination as vertical axis is called 'the Interferogram'. (Fig. 4) Here it will be referred to as 'the Interferogram Cloud' that the intensity of interference is distributed in the 3D space.

Fig. 1: A photograph of the BW-S507 system

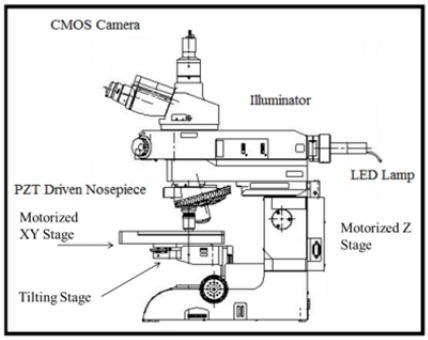

Fig. 2: A feature drawing of the microscope dedicated to the BW-S507.

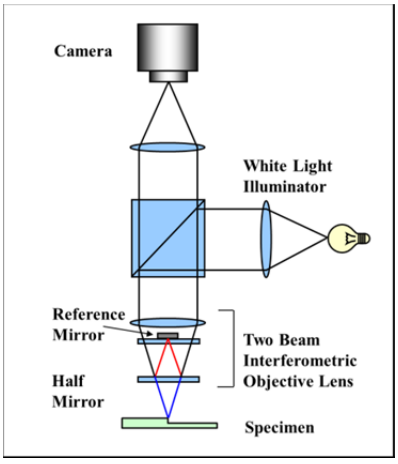

Fig. 3: A concept drawing of the White Light Interferometry

2.2 The algorithm for the point focus sharpness [6]

The context to get surface topography is described as follows: first, the voxel operator, which is defined as Fig. 5, is applied to the Interferogram Cloud. Then the Point Focus Sharpness (hereinafter, abbreviated as PFS) is calculated. The z coordination that gives the maximum of PFS for each pixel becomes the surface height of the pixel. The voxel operator shown in Fig. 5 is explained here. Each element value of the center 3X3 matrix is a numerical weight of the pixel of interest A and the adjacent pixels. It is possible to set numerical weights for the matrix U and the matrix L which is located at the upper layer or lower layer from the center layer by a distance L respectively. The L is decided as about a half of wave length of the Interferogram. The PFS is calculated by Eq. (1).

$$PFS = \sum_{i=1}^{27}(w_i I_i) \quad (1)$$
$$w_i = numerical\ weight$$
$$I_i = Image\ pixel\ data$$

Since different weight patterns of voxel operate to the primary surface and then generate different PFS values so these voxel operators will be referred to as the Digital Stylus by an analogy of stylus profiler. The Cone and the Point, which are names of the Digital Stylus as shown in the Fig. 6, are examined for both super smooth surface and very rough surface. The Cone has a function of the FV while the Point has no function of the FV. The first test is made for the SiC wafer, which has 0.1nm class super smooth surface. Consequently 32 height images of the same field of view are acquired. First half of height images and second half of height images are cumulated respectively then two average height images are made. The standard deviation value of the subtracted image between the above two images is evaluated as a system noise level for each pixels. The subtracted images are shown in Fig. 7. The value for the Cone is 39.8 pm, the value for the Point is 40.8 pm. There is no significant difference between the two Digital Styluses for the super smooth surface. Next these two patterns are applied to the very rough surface of ceramics substrate. The two surface topographies are shown in Fig. 8. Visually the height image by the Cone is better than the height image by the Point.

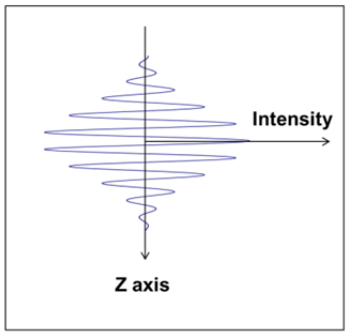

Fig. 4: The Interferogram

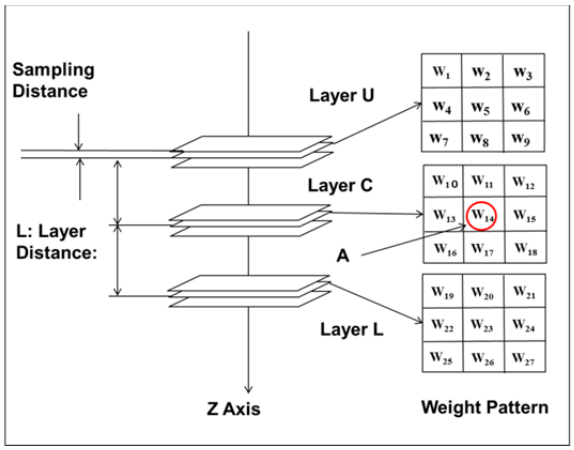

Fig. 5: The Voxel Operator for the PFS calculation

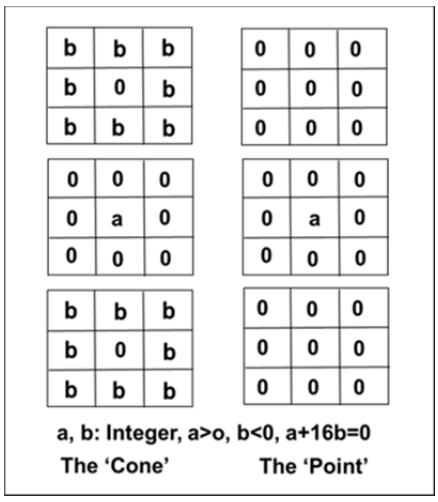

Fig. 6: The Digital Styluses tested

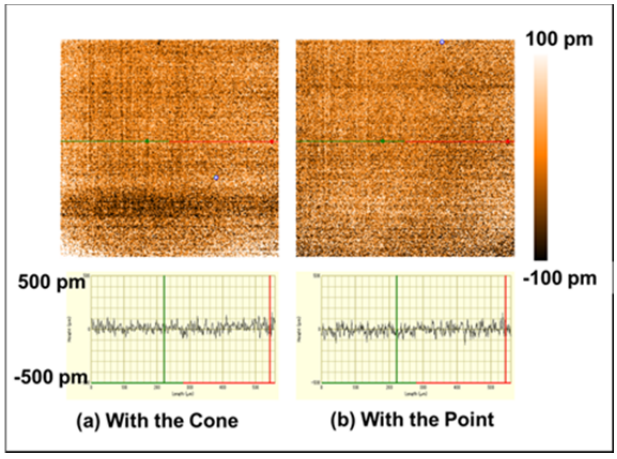

Fig. 7: System noise images

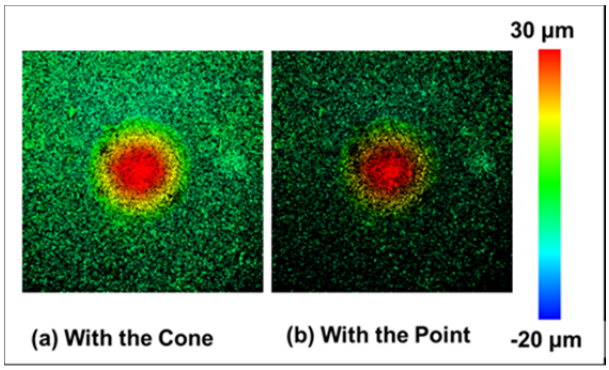

Fig. 8: Surface topographies for the rough surface.

2.3 Algorithm for deciding of focal point [7]

In this section the algorithm for deciding the peak of the interferogram with very high resolution of 1 pico meter is described. A plot of the values of the PFS with respect to sampling point z_i on the z axis is shown in Fig. 9. Scanning along the z-axis completes sequence data of PFS about a point on the z-axis giving the maximum value of PFS. These sequence data for each pixels are stored. The function form g(z) similar to the data point sequence is determined in advance. The APF shown in Eq. (2) is defined by introducing a shift variable of 'a'.

$$APF = \partial \left(\sum_{i=1}^{n} (D_i g(zi - a)) \right) / \partial a \qquad (2)$$

z_i: z coordination of sampling point
D_i: PFS value
n: a number of sampling points
a: a shifting variable
g(z): a fixed function

The APF for z in the direction approaching the focal point z_0 is positive. The APF for z in the direction departing from the focal point z_0 is negative. A shift amount of the point at which the APF is zero is a shift amount from the z-coordination of point at which the PFS value is maximum based on the sampling. When Eq. (3) cannot be solved analytically, it is possible to use the Newton's method for solving in the numerical operation. As 1 pico meter is set for the truncation error of Newton's method the system can calculate the surface topography with 1 pico meter vertical resolution.

$$APF(a) = 0 \qquad (3)$$

The process of the Newton's Method is shown in Fig. 10.

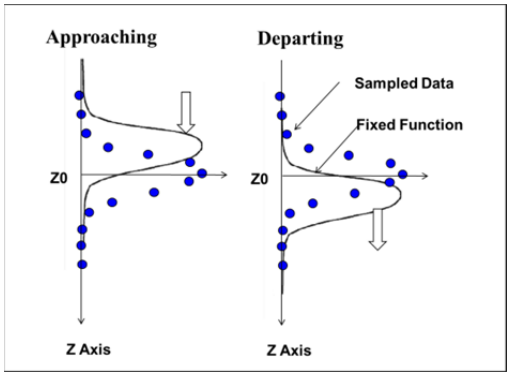

Fig. 9: The APF: Approaching Function

Table 1: Specification of the experimented system

Item	Specification
System Type	BW-S507
Camera	CMOS(USB3.0) 2046X2046 or 1022X1022
PC	High Performance Type for BW series
Monitor	27" Wide
XY Stage	Ultra Sound Motor Drive 130mm x 85mm
Z Stage	Motorized (travel 20mm)
Z Actuator	Nosepiece Driven PZT Actuator
Microscope	Type BW-FMA
Objective Lens	Two Beam Interferometric Objective Lens 2.5X, 5X, 10X, 20X, 50X, 100X

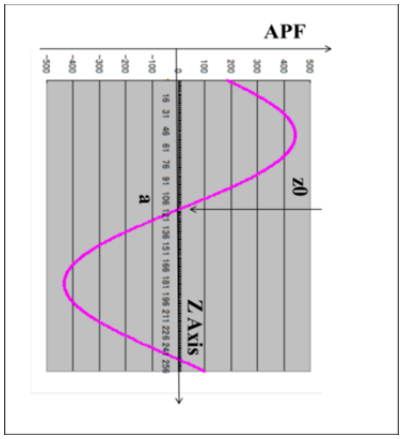

Fig. 10: The process of the Newton's method

3. EXPERIMENTS

3.1 Traceability

The repeatability is tested with an 8nm VLSI Step Height Standards sample, certified by NIST. All the following experiments are done using the BW-S507 system; the specifications are shown in Table 1. The installation environment is in the fourth floor of an 11-story office building; the floor is a concrete slab. An active type vibration isolator is used. For this traceability test the 20x double beam interference objective lens is used, so as to measure the area of 556 μm x 556 μm. The surface topography data is shown in Fig. 11. The Table 2 shows the data for 10 measurements, average and standard deviation. The mean value and each of the 10 data are within the uncertainty range. The repeatability (σ) is 0.0979 nm.

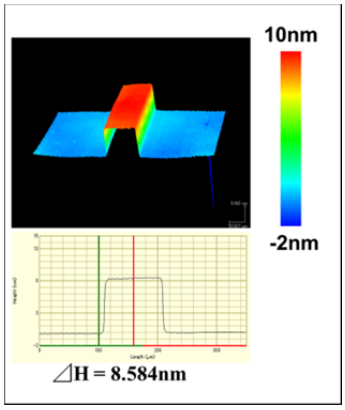

Fig. 11: A surface topography of the Step Height Standard

Table 2: The repeatability test for the Step Height Standard

N	Step Height
1	8.4072 nm
2	8.5038 nm
3	8.4838 nm
4	8.6646 nm
5	8.5327 nm
6	8.4203 nm
7	8.7174 nm
8	8.5706 nm
9	8.5844 nm
10	8.5492 nm
Mean	8.5434 nm
Std. dev.	0.0979 nm
Std. dev./Mean	1.146 %

3.2 Independency on a wavelength of the interferogram

It is not necessary to consider a fluctuation of the illuminating light source because this algorithm doesn't require a wavelength λ of the interferogram. To demonstrate this capability, step height data are measured with a wavelength of the interferogram as a parameter during from turning on the LED light source to 10000 minutes elapsed time later. The result data are shown in Table 3 and Fig. 12. The linear regression analysis between a wavelength and step height is done. The Linear Regression Evaluation Coefficient R^2 is 0.0115. This suggests that these two parameters have no relationship.

Table 3: The relationship with the wavelength and step height

Elapsed Time (min)	Wave Length (nm)	Step Height (nm)
1	278.1	8.871
10	282.4	8.806
100	282.2	8.605
1000	281.7	8.799
10000	278.9	8.593
Ave.	280.7	8.735
Std.	2.012	0.127

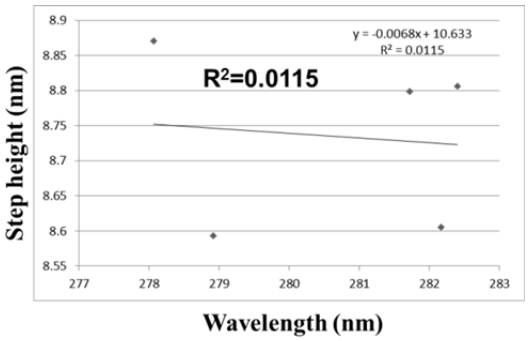

Fig. 12: The step height vs the wavelength

3.3 Independency on magnification of the objectives.

The larger NA: Numerical Aperture is a cause of shorter wavelength of the interferogram. The system used the algorithm which is based on a phase angle of the interferogram it required height calibrations for all objective lenses installed. For this system, calibration free capability of objective lens is realized. To demonstrate this feature, the VLSI standard sample is measured with 2.5X, 5X, 10X, 20X, 50X and 100X objective lenses. The average step height is calculated by 10 measurements for each objective lens. The result data are shown in Table 4 and Fig. 13. The linear regression analysis between NA and step height is done. The Linear Regression Evaluation Coefficient R^2 is 0.00001. This suggests that these two parameters have no relationship.

Table 4: The relationship with the NA and step height

Lens Mag.	NA	Step Height (nm)
2.5X	0.075	8.595
5X	0.130	8.894
10X	0.300	8.642
20X	0.400	8.543
50X	0.550	8.615
100X	0.700	8.801

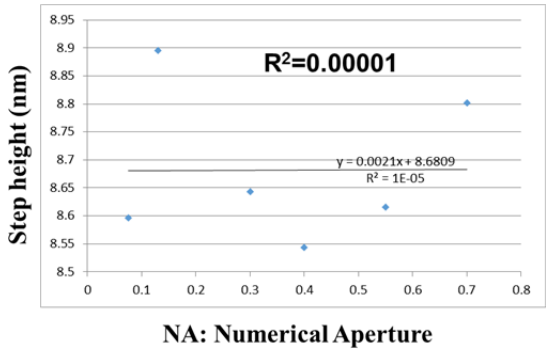

Fig. 13: The step height vs NA

4. APPLICATIONS

4.1 Super Smooth Surface

SiC wafer, CMP: Chemical Mechanical Planarization wafer and glass substrate, etc. these materials are very important for the Power Semiconductor, 3D IC and MEMS applications. The Sa: mean height of the surface for the above materials is less than 0.2 nm in general. In such a case, the reference surface correction is required. Fig. 14 (a) is an original surface topography of SiC wafer; (b) is the reference surface topography. The corrected surface of SiC wafer (c) is created by subtraction of the reference surface image from the original surface image. In Fig. 15, surface profiles are shown.

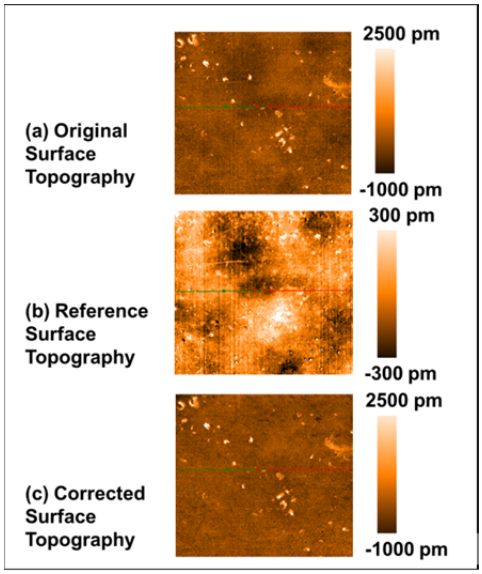

Fig. 14: Surface topography of SiC wafer.

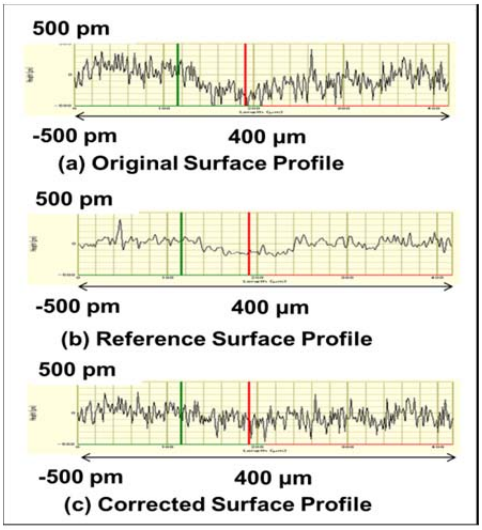

Fig. 15: Surface Profiles of the SiC wafer

4.2 Nano height patterned surface

The height evaluation for Nanomaterials such as the Graphene Layer, the Graphite Monolayer, the Self-Assembled Monolayer and MoS_2 Monolayer, is needed. In Fig. 16 the surface topography of the 8nm class VLSI Step Height Standards is shown as an example of nano height patterned surface.

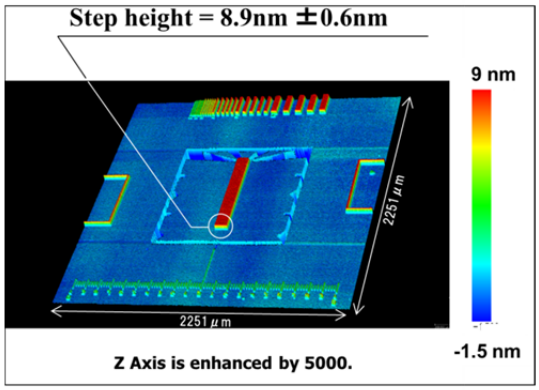

Fig. 16: 8nm class VLSI Step Height Standard

4.3 Rough surface

Ceramics IC package, sheet, knife Zirconia, ceramics parts and Turbine Blade, these ceramics materials are also applied for surface roughness and geometric measurement of structure, such as bump, dent and hemisphere. In Fig. 17 the surface topography of a ceramics bump is shown.

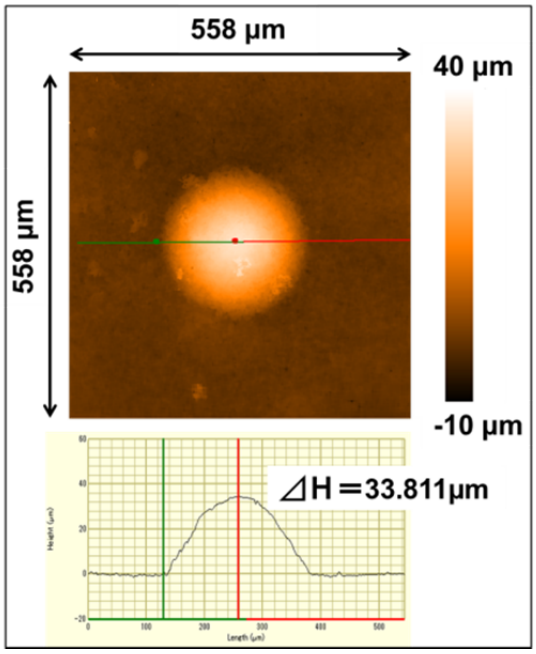

Fig. 17: Ceramic bump

5. CONCLUSION

In this paper, the FVWLI method is newly introduced. This method is composed of two core algorithms. The first developed algorithm is the Digital Stylus, which is named in the voxel operator. This is a technique to improve an ability to capture rough surface of the WLI. The second developed and most important algorithm is the APF. The FVWLI is independent on a wavelength of the interferogram, whereas the conventional WLI depends on it. And the vertical resolution defined by the algorithm is achieved 1 picometer. It also introduced a system equipped with these algorithms. The system is widely applicable to a field of R&D for materials science, such as SiC wafer, CMP wafer, glass substrate, Graphene, ceramics, and so on.

ACKNOWLEDGEMENTS

The author would like to thank Prof. Kazuhisa Yanagi, Nagaoka University of Technology for advice on surface metrology. I would also like to thank Mr. Takao Koga and members of the team of BW, Instruments Company, Nikon Corporation for the artistic measurement results.

REFERENCES

[1] R. Danzl, F. Helmli, S. Scherer, 'Focus variation – a new technology for high resolution optical 3D surface metrology', Proc. 10th Int. Conf. of the Slovenian Society for Non-Destructive Testing, pp. 481-491, Ljubljana, Slovenia, Sep. 2009.

[2] B. Bhushan, J. C. Wyant and C. L. Koliopoulos, "Measurement of surface topography of magnetic tapes by Mirau interferometry", *Appl. Optics,* vol. 24, No. 10, pp. 1489-1497, May 1985..

[3] P. de Groot and L. Deck, "Surface profiling by analysis of white light interferograms in the spatial frequency domain", *J. of Mod. Opt.*, vol. 42, pp. 389 - 401, 1995.

[4] A. Harasaki, J. Schmit and J. C. Wyant, "Improved vertical-scanning interferometry", *Appl. Optics,* vol. 39, No. 13, pp. 2107 - 2115, May 2000.

[5] D. Mansfield and A. Bankhead, "Apparatus for and a method of determining a surface characteristic", *US Patent,* US 20060176522 A1, Aug. 2006.

[6] T. Nishikawa, "Shape measurement device, observation device and image processing method", *Int. Patent Appl.* WO2010/134343 A1, Nov. 2010.

[7] T. Nishikawa, "Height measuring method and height measuring device", *Int. Patent Appl*. WO2011/138874 A1, Nov. 2011.